

# Primordial density and BAO reconstruction

Hong-Ming Zhu,<sup>1,2</sup> Ue-Li Pen,<sup>3,4,5,6</sup> Matthew McQuinn,<sup>7</sup> and Xuelei Chen<sup>1,2,8</sup>

<sup>1</sup>*Key Laboratory for Computational Astrophysics, National Astronomical Observatories, Chinese Academy of Sciences, 20A Datun Road, Beijing 100012, China*

<sup>2</sup>*University of Chinese Academy of Sciences, Beijing 100049, China*

<sup>3</sup>*Canadian Institute for Theoretical Astrophysics, University of Toronto, 60 St. George Street, Toronto, Ontario M5S 3H8, Canada*

<sup>4</sup>*Dunlap Institute for Astronomy and Astrophysics, University of Toronto, 50 St. George Street, Toronto, Ontario M5S 3H4, Canada*

<sup>5</sup>*Canadian Institute for Advanced Research, CIFAR Program in Gravitation and Cosmology, Toronto, Ontario M5G 1Z8, Canada*

<sup>6</sup>*Perimeter Institute for Theoretical Physics, 31 Caroline Street North, Waterloo, Ontario, N2L 2Y5, Canada*

<sup>7</sup>*Department of Astronomy, University of Washington, Seattle, WA 98195, USA*

<sup>8</sup>*Center of High Energy Physics, Peking University, Beijing 100871, China*

(Dated: August 24, 2016)

In this paper we introduce a new way to reconstruct BAO peaks in real space.

PACS numbers:

## I. INTRODUCTION

The standard BAO reconstruction uses the negative Zel'dovich (linear) displacement to reverse the large-scale bulk flows [1]. The nonlinear density field is usually smoothed on the linear scale ( $\sim 10$  Mpc/ $h$ ) to make the Zel'dovich approximation valid. Actually, the fully nonlinear displacement which describes the motion beyond the linear order (the Zel'dovich approximation) can be solved from the nonlinear density field. While the algorithm is complicated in the three spatial dimensions, it is quite simple in the 1D case, which is basically the ordering of mass elements. The 1D cosmological dynamics corresponds to the interaction of infinite sheets of matter where the force is independent of distance [2]. These sheets are moving in a Hubble flow relative to one another and the surface density in each sheet scales as  $a^{-2}$ . The simplified 1D dynamics provides an excellent means of understanding the structure formation and testing perturbation theories [2]. In this paper we solve the fully nonlinear displacement in 1D and present a new method to reconstruct the primordial density field and hence the linear BAO information.

This paper is organized as follows. In Section II, we briefly describe the 1D  $N$ -body simulation. In Section III, we present the reconstruction algorithm in the 1D case. In Section IV, we show the results of reconstruction. In Section V, we discuss the 3D case and future improvements.

## II. SIMULATIONS

To simulate the gravitational dynamics in 1D, we use the 1D particle-mesh (PM) code in Ref. [2]. The 1D simulation we use involves  $3 \times 10^8$  sheets with  $3 \times 10^8$  PM elements in a  $10^8$  Mpc box. The initial condition is generated using the Zel'dovich approximation. Since the

Zel'dovich approximation is exact up to shell crossing, we start the PM calculation at  $z = 10$ . In the analysis, we use the output at  $z = 0$ . We scale the initial density field by the linear growth factor to get the linear density field at  $z = 0$ .

## III. RECONSTRUCTION ALGORITHM

The Lagrangian displacement  $\Psi(q)$  fully describes the motion of mass elements. The Eulerian position  $x$  of a mass element is

$$x = q + \Psi(q), \quad (1)$$

where  $q$  is the initial Lagrangian position of this mass element. In the simulations, mass elements (sheets) are labeled by their initial Lagrangian coordinates. Once we know their Eulerian positions, the displacement field is obtained. Observationally, we only have the unlabelled Eulerian coordinates. The estimated displacement at the Lagrangian coordinate  $q = iL/N$  is

$$s(q) = x_i - iL/N, \quad (2)$$

where we have ordered the sheet labels  $i$  from left to right,  $L$  is the box size, and  $N$  is the sheet number. If no shell crossing happens, the reconstructed displacement is exact up to a global shift. In the nonlinear regime once shell crossing occurs, the estimated displacement field is quite noisy on the scale  $L/N$ . To reduce stochasticities in the estimated displacement field, we can use the averaged displacement of  $n_p$  particles

$$s(q) = \frac{1}{n_p} \sum_{j=i}^{i+n_p-1} x_j - in_p L/N, \quad (3)$$

where  $q = in_p L/N$  and  $j$  is the sheet label. Here  $i$  varies from 0 to  $N/n_p$  and  $j$  varies from 0 to  $N$ .

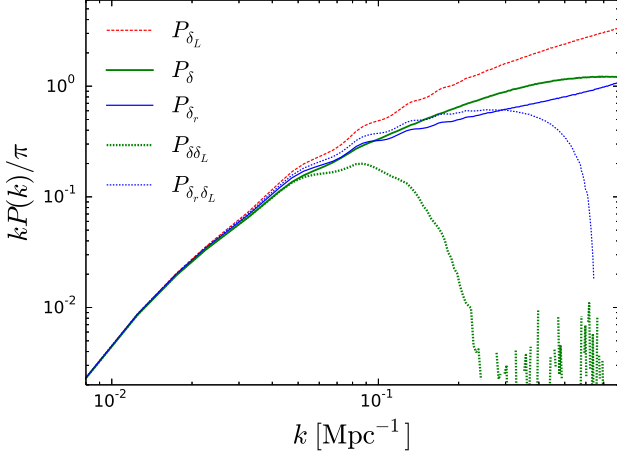


FIG. 1: The power spectra of the linear (dashed line), nonlinear (thick solid line), and reconstructed (thin solid line) fields. We also plot the nonlinear-linear (thick dotted line) and reconstructed-linear (thin dotted line) cross-correlation power spectra. The wiggles in the reconstructed power spectrum are also much more transparent than the nonlinear power spectrum.

The derivative (actually the divergence) of  $s(q)$  gives the reconstructed density field

$$\delta_r(q) = -\frac{\partial s(q)}{\partial q}, \quad (4)$$

i.e., the differential motion of mass elements. [is this argument appropriate? shall we discuss more here?](#) Reconstruction from the gridded density field can be implemented following the same principle, which we adopt in the following calculations.

#### IV. RESULTS

Figure 1 shows the linear, nonlinear and reconstructed power spectra, as well as the cross-correlation power spectra. The correlation of the reconstruction density field  $\delta_r$  with the linear density field  $\delta_L$  is much better than that of the raw nonlinear density field  $\delta$ . The wiggles in the reconstructed power spectrum are also much more transparent than the nonlinear power spectrum. The nonlinear density field  $\delta(x)$  is given on the Eulerian position  $x$ , while the reconstructed density field  $\delta_r(q)$  is calculated on the Lagrangian position  $q$ .

To conveniently quantify the linear information  $\delta_L$  in the nonlinear density field  $\delta$ , we decompose the nonlinear density field  $\delta$  as

$$\delta(k) = b(k)\delta_L(k) + n(k). \quad (5)$$

Here,  $b\delta_L$  is completely correlated with the linear density field  $\delta_L$ . Correlating the nonlinear density field with the linear density field,

$$\langle \delta(k)\delta_L(k) \rangle = b(k)\langle \delta_L(k)\delta_L(k) \rangle, \quad (6)$$

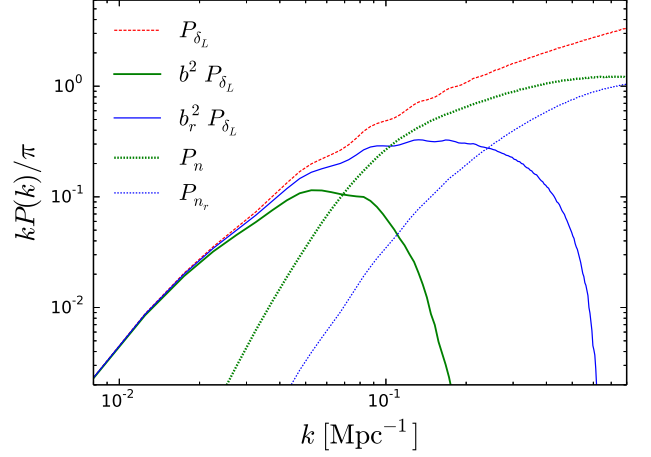


FIG. 2: The linear power spectrum (dashed line), the linear components in the nonlinear (thick solid line) and reconstructed (thin solid line) fields, the noise parts of the nonlinear (thick dotted line) and reconstructed (thin dotted line) fields. The noise terms dominate over the signals at  $k \gtrsim 0.07 \text{ Mpc}^{-1}$  for the nonlinear field and  $k_q \gtrsim 0.24 \text{ Mpc}^{-1}$  for the reconstructed field.

we obtain

$$b(k) = \frac{P_{\delta\delta_L}(k)}{P_{\delta_L}(k)}. \quad (7)$$

Nonlinear evolution drives  $b$  to drop from unity, reducing the linear signal. Separating the part correlated with the linear density field, we then have

$$n(k) = \delta(k) - b(k)\delta_L(k). \quad (8)$$

$n$  is generated in the nonlinear evolution and thus uncorrelated with the linear density field  $\delta_L$ , further reducing  $b\delta_L$  with respect to  $\delta$ . This part induces noises in the measurement of BAO. Such decomposition helps to write the nonlinear power spectrum as

$$P_\delta(k) = b^2(k)P_{\delta_L}(k) + P_n(k). \quad (9)$$

Here,  $b(k)$  is often referred as the “propagator” and  $P_n$  is usually called the mode-coupling term [3–5]. For the reconstructed field  $\delta_r(q)$ , we also have

$$\delta_r(k_q) = b_r(k_q)\delta_L(k_q) + n_r(k_q), \quad (10)$$

where

$$b_r(k_q) = \frac{P_{\delta_r\delta_L}(k_q)}{P_{\delta_L}(k_q)}. \quad (11)$$

The reconstructed power spectrum is

$$P_{\delta_r}(k_q) = b_r^2(k_q)P_{\delta_L}(k_q) + P_{n_r}(k_q). \quad (12)$$

Here, the subscript “ $q$ ” denotes that the reconstructed field is given on the Lagrangian coordinate. In Fig. 2 we

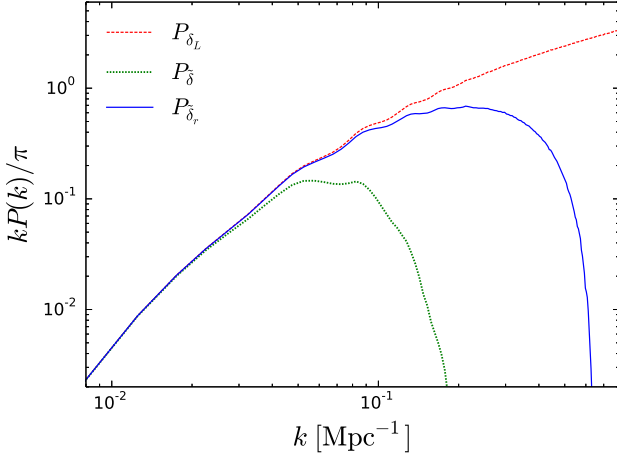


FIG. 3: The power spectra for the linear (dashed line), filtered nonlinear (dotted line) and filtered reconstructed (solid line) fields.

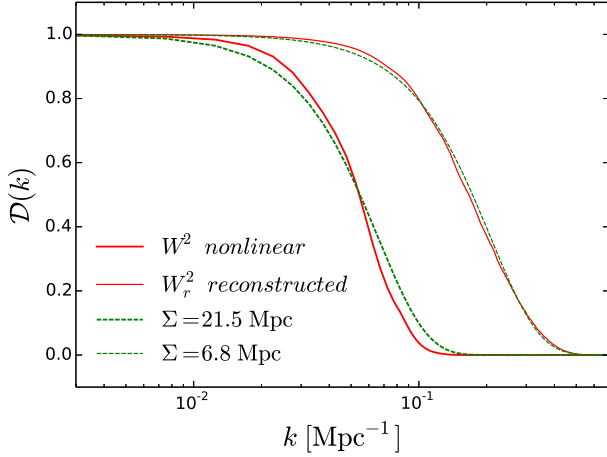


FIG. 4: The damping factors for the nonlinear (thick solid line) and reconstructed (thin solid line) fields. The Gaussian BAO damping models with  $\Sigma = 21.5$  Mpc (thick dashed line) and  $\Sigma = 6.8$  Mpc (thin dashed line).

plot the linear components and the noise terms of the nonlinear and reconstructed fields.

The raw reconstructed field  $\delta_r$  is still noisy on small scales ( $k_q \gtrsim 0.24 \text{ Mpc}^{-1}$ ). To optimally filter out the noise from the raw reconstructed field, we use the Wiener filter

$$W_r(k_q) = \frac{P_{\delta_L}(k_q)}{P_{\delta_L}(k_q) + P_{n_r}(k_q)/b_r^2(k_q)}. \quad (13)$$

Deconvolving  $b_r$  and using the Wiener filtering, we obtain the optimal reconstructed field,

$$\tilde{\delta}_r(k_q) = \frac{\delta_r(k_q)}{b_r(k_q)} W_r(k_q). \quad (14)$$

The power spectrum of the optimal reconstructed field

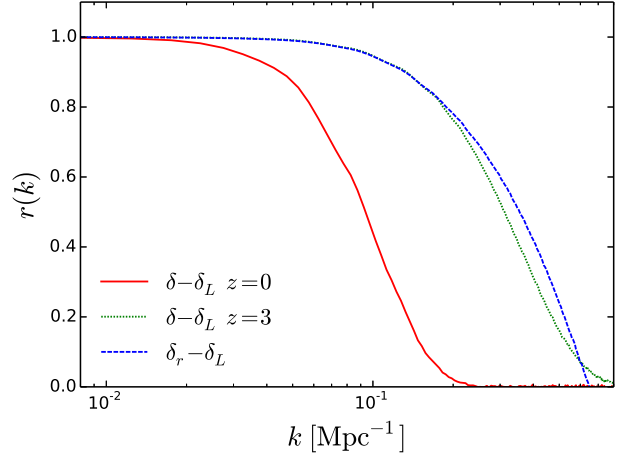


FIG. 5: The  $\delta - \delta_L$  correlation coefficients at  $z = 0$  (solid line) and  $z = 3$  (dotted line), as well as the  $\delta_r - \delta_L$  correlation coefficient (dashed line).

$\tilde{\delta}_r$  is given by

$$P_{\tilde{\delta}_r}(k_q) = W_r^2(k_q)P_{\delta_L}(k_q) + W_r^2(k_q)P_{n_r}(k_q)/b_r^2(k_q), \quad (15)$$

where  $W_r^2$  describes the damping of the linear power spectrum. The raw nonlinear field  $\delta$  is also filtered. In Fig. 3, we plot the power spectra of the optimal reconstructed and nonlinear fields.

Figure 4 shows the damping factors for the optimal filtered nonlinear and reconstructed fields. The damping of the linear power spectrum is significantly reduced after reconstruction. We also overplot the best-fitting Gaussian BAO damping model,

$$\mathcal{D}(k) = e^{-k^2 \Sigma^2 / 2}, \quad (16)$$

with  $\Sigma = 21.5$  Mpc and 6.8 Mpc for the nonlinear and reconstructed fields. The new BAO reconstruction algorithm reduces the the nonlinear damping scale  $\Sigma$  by 60 per cent, i.e., a factor of three. The damping factor is above 0.8 for  $k \lesssim 0.1 \text{ Mpc}^{-1}$ . However, the 100 per cent reconstruction, cancelling any nonlinear effects, is still unachievable, as some information has been irreversibly lost.

Reconstruction reduces the nonlinear damping  $\mathcal{D}$  as well as the noise term  $P_n$ . To quantify the overall performance, we can use the cross-correlation coefficient

$$r(k) = \frac{P_{\delta\delta_L}(k)}{\sqrt{P_{\delta}(k)P_{\delta_L}(k)}} = \frac{1}{\sqrt{1 + \eta(k)}}, \quad (17)$$

where  $\eta = P_n/(b^2 P_{\delta_L})$  quantifies the relative amplitude of  $n$  with respect to  $b\delta_L$ . We plot the cross-correlation coefficients in Fig. 5. The correlation of  $\delta_r$  with  $\delta_L$  is as good as that of  $\delta$  at  $z = 3$ .

The density fluctuation probability distribution function (PDF) quantifies the Gaussianity of the density field. Figure 6 shows the PDFs of the nonlinear and reconstructed density fields. We also plot the PDFs of the

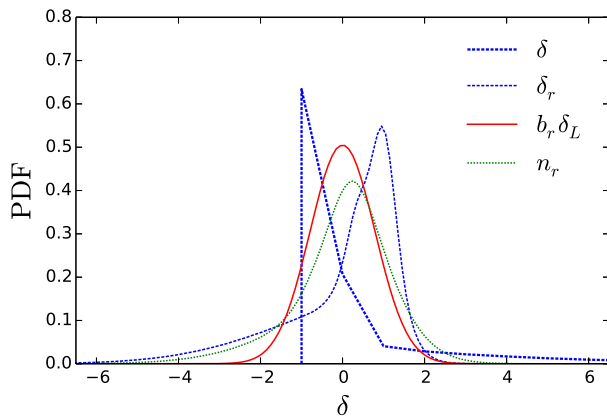


FIG. 6: The probability distribution functions of the nonlinear (thick dashed line) and reconstructed (thin dashed line) fields. We also show the probability distribution functions of the linear component (solid line) and the noise part (dotted line).

linear component  $b_r \delta_L$  and the noise part  $n_r$  of the reconstructed density field  $\delta_r$ . Of course the linear component is Gaussian, while the noise part is nonGaussian. As a result, the reconstructed density field is also nonGaussian. The raw nonlinear density field is significantly nonGaussian.

## V. DISCUSSIONS

In reality, the Universe is 3D instead of 1D.

The new method significantly improves the expansion rate measurement from BAO. (more discussions?)

This method can be generalized to the 3D case. We leave this to future work.

Comparison with and Implications for the standard BAO reconstruction: exact Lagrangian displacement, nonlinear displacement, which is easier to model.

If use the displacement solved in this paper for the standard BAO rec, we expect the performance will become much better but still not as good as our results.

## VI. ACKNOWLEDGEMENT

We thank Yu Yu and Tian-Xiang Mao for helpful discussions. We acknowledge the support of the Chinese MoST 863 program under Grant No. 2012AA121701, the CAS Science Strategic Priority Research Program XDB09000000, the NSFC under Grant No. 11373030, IAS at Tsinghua University, and NSERC. The Dunlap Institute is funded through an endowment established by the David Dunlap family and the University of Toronto. Research at the Perimeter Institute is supported by the Government of Canada through Industry Canada and by the Province of Ontario through the Ministry of Research & Innovation.

- 
- [1] D. J. Eisenstein, H.-J. Seo, E. Sirko, and D. N. Spergel, *ApJ* **664**, 675 (2007), astro-ph/0604362.
  - [2] M. McQuinn and M. White, *J. Cosmology Astropart. Phys.* **1**, 043 (2016), 1502.07389.
  - [3] M. Crocce and R. Scoccimarro, *Phys. Rev. D* **73**, 063520

- (2006), astro-ph/0509419.
- [4] M. Crocce and R. Scoccimarro, *Phys. Rev. D* **77**, 023533 (2008), 0704.2783.
- [5] T. Matsubara, *Phys. Rev. D* **77**, 063530 (2008), 0711.2521.